Multidecadal variations of Fremantle sea level: Footprint of climate variability in the tropical Pacific

Ming Feng,[1] Yun Li,[2] and Gary Meyers[3]

Received 10 March 2004; accepted 21 July 2004; published 18 August 2004.

[1] Coastal sea level at Fremantle, Western Australia is strongly influenced by trade wind variations in the tropical Pacific, due to the existence of equatorial and coastal wave guides. Corroborated with low-pass filtered Southern Oscillation Index (SOI-M), Pacific Decadal Oscillation (PDO) causes high Fremantle sea levels during positive SOI-M regimes (with more frequent La Niña events) and low sea levels during negative SOI-M regimes (with more frequent El Niño events), due to enhanced and slackened trade winds. The multidecadal variation of the Fremantle sea level obscures its long-term rising trend during the 1950's to mid 1990's. Statistical regression models are used to describe relationships between the multidecadal sea level variation and SOI-M, in an attempt to separate natural climate variability and climate change effects. A non-parametric regression model reveals a nonlinear relationship, likely due to different responses of the sea level (upper-ocean) to the El Niño and La Niña events. *INDEX TERMS:* 4556 Oceanography: Physical: Sea level variations; 4215 Oceanography: General: Climate and interannual variability (3309); 4231 Oceanography: General: Equatorial oceanography. **Citation:** Feng, M., Y. Li, and G. Meyers (2004), Multidecadal variations of Fremantle sea level: Footprint of climate variability in the tropical Pacific, *Geophys. Res. Lett.*, *31*, L16302, doi:10.1029/2004GL019947.

1. Introduction

[2] Fremantle (32°03′S, 115°44′E), situated at the south-west coast of the Australian continent, is a major port in the Indian Ocean (Figure 1). Sea level has been recorded at Fremantle since 1897, which is the longest in the southern hemisphere. Glacial isostatic adjustment and tectonic contribution to the Fremantle sea level are small [*Lambeck*, 2002], and the effect of local land movements on the sea level variations is negligible (M. Eliot and C. Pattiaratchi, personal communication, 2003). Thus, the Fremantle sea level is a useful index for long-term climate variability and climate change research.

[3] Interannual upper ocean anomalies in the tropical Pacific, mostly caused by trade wind variations related to El Niño/Southern Oscillation (ENSO), propagate westward as equatorial Rossby waves, and then poleward along the northwest to western Australian coast as coastally-trapped waves. These waves transmit deep thermoclines and high coastal sea level anomalies (SLA) during La Niña years and shallow thermoclines and low SLA during El Niño years [*Pariwono et al.*, 1986; *Meyers*, 1996; *Feng et al.*, 2003; *Holgate and Woodworth*, 2004]. This relationship can be understood using vertically integrated momentum equation along the waveguides (Figure 1a) at low-frequency, in which the balance between the pressure gradient and wind stress dominates [*Godfrey*, 1996],

$$\partial P/\partial l = \tau^l/g\rho_0 \quad (1)$$

Here $P = \int_{-Z}^{0} \varsigma dz$, Z (~2000 m) is the maximum sill depth in the Indonesian seas, ς is the steric height anomaly relative to $-Z$, and g and ρ_0 are the acceleration due to gravity and surface density, respectively.

[4] Multidecadal variability of ENSO, or Pacific Decadal Oscillation (PDO), has received great attention in recent years [*Gu and Philander*, 1995; *Zhang et al.*, 1997]. There are more frequent El Niño (La Niña) events during 1977–1997 (1955–1975), causing a multidecadal trade wind anomaly (Figure 1a). Thermocline depth anomaly related to the PDO (Figure 1b), which is similar to the ENSO asymmetry pattern [*Rodgers et al.*, 2004], induces a multi-decadal variation of the Fremantle SLA (Figure 2).

[5] A long-term rising trend of 1.54 mm per year in the Fremantle sea level (Figure 2a) corresponds to a warming trend in the global average surface temperature (Figure 2c). This rising trend is not obvious during the decades from 1950's to mid 1990's due to the multidecadal variation. *Church et al.* [2004] also found that the sea level rising trends in the tropical western Pacific to eastern Indian Ocean are lower than the global average over the 1950 to 2000 period. Thus, to better quantify the sea level rise, there is a need to separate the sea level variations due to climate variability and climate change.

[6] In this study, statistical models are used to describe relationships between detrended low-frequency Fremantle SLA and low-frequency Southern Oscillation Index (SOI) variations, in an attempt to separate the natural climate variability effect from the sea level rise. We find out that the low-frequency SOI explains a significant portion of the Fremantle SLA, though other climate signals in the Indian Ocean [e.g., *Allan et al.*, 1995; *Feng and Meyers*, 2002] may also contribute.

2. Multidecadal Variations of the Fremantle Sea Level and SOI

[7] Power spectrum of the Fremantle SLA has both interannual and multidecadal peaks (Figure 2d), with a natural spectrum gap at near 20 years, so that we use a 19-year Hanning filter to separate the multidecadal signals.

[1]CSIRO Marine Research, Floreat, Western Australia, Australia.
[2]CSIRO Mathematical and Information Sciences, Wembley, Western Australia, Australia.
[3]CSIRO Marine Research, Hobart, Tasmania, Australia.

0094-8276/04/2004GL019947$05.00

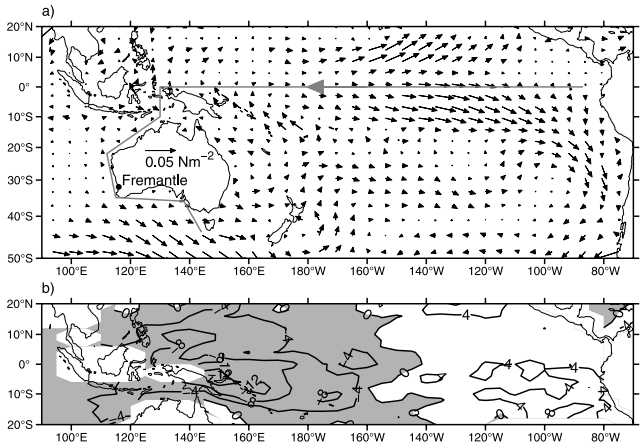

Figure 1. (a) Surface wind stress differences between 1977–1997 and 1955–1975 from NCEP reanalysis data [*Kalnay et al.*, 1996], and (b) 20°C isothermal depth differences between 1955–1975 and 1977–1997 using *White and Bernstein* [1979] upper ocean thermal data. In (a), the location of Fremantle is denoted and the light line sketches the integrating path along the equatorial and coastal waveguides.

Later on we use SLA-M to represent the detrended, low-pass filtered annual mean Fremantle SLA (Figure 2e), and SOI-M to represent the low-pass filtered annual mean SOI (Figure 2f).

[8] There is significant negative correlation between the SOI-M and the low-pass filtered PDO index (Figure 2f), defined from North Pacific sea surface temperature [*Zhang et al.*, 1997]. The PDO index tends to lead the opposite SOI-M peaks by three years, with a peak correlation of −0.85 at the 99% significance level. From the early 1950's to mid-1970's, the SOI-M is positive when there are more La Niña events than El Niño events (Figure 2f), and this period is called a positive SOI-M regime; and from the mid-1970's to mid-1990's, the SOI-M is negative when there are more El Niño events than La Niña events, and it is called a negative SOI-M regime. There is another apparent phase transition to a positive SOI-M regime since the 1997/98 ENSO event, and two other phase transitions early during the century.

[9] Linear correlation between the SLA-M and SOI-M is rather high, 0.83 at 99% significance level. The positive SLA-M from the early 1950's to mid 1970's and negative SLA-M during mid 1970's to mid 1990's are due to PDO influence (Figure 2e). The correlation is not clear before the 1920's, when the gaps in the Fremantle sea level data are rather large (Figure 2b). We use data after 1922 in next two sections to quantify statistical relationships between the SLA-M and SOI-M.

3. Linear Regression Between SLA-M and SOI-M

[10] To separate the natural climate variability signals in the SLA-M, we use the SOI-M as an index for the low-frequency equatorial Pacific wind. The SOI is closely correlated with average zonal wind stress along the equatorial Pacific on both interannual and multidecadal time scales (Figure 2f), with an overall correlation of 0.8.

[11] First a linear regression is applied between the two variables with a structural model [*Zheng et al.*, 1997]

$$Y_t = 3.96 + 5.34X_t + \varepsilon_t \quad (2)$$

where X_t is the SOI-M and ε_t is the residual, a fourth order autoregressive process (Figure 3). 69% of variance of the

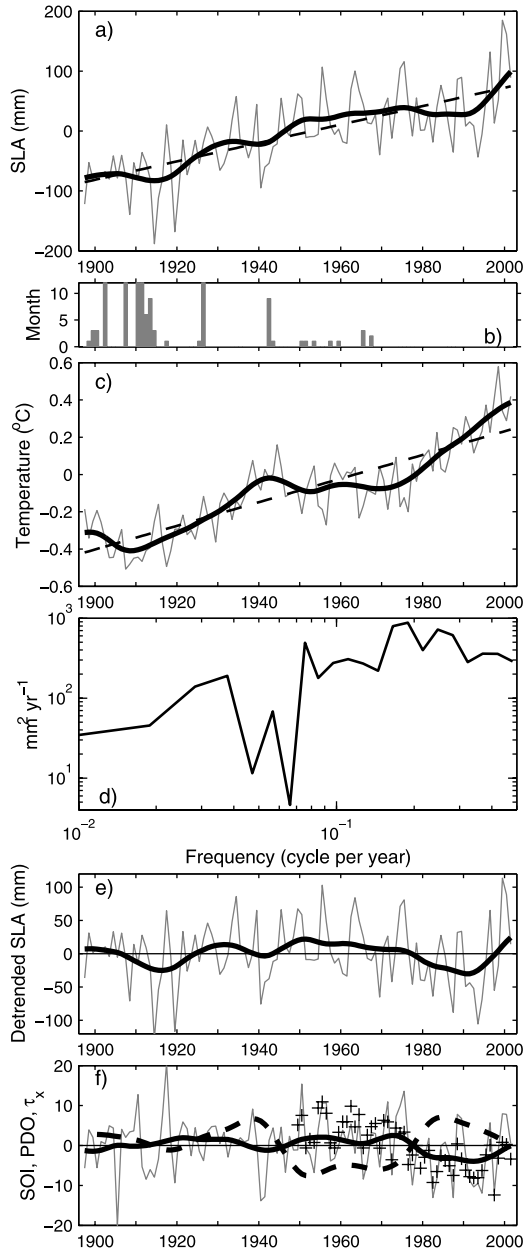

Figure 2. (a) Annual mean Fremantle SLA, (b) numbers of months with missing sea level data, (c) global average surface temperature [*Jones et al.*, 1999], (d) power spectrum of the SLA, (e) annual mean detrended SLA, and (f) annual mean SOI and average easterly wind stress anomaly at the equatorial Pacific (crosses, unit: 10^{-3} Nm^{-2}). The heavy lines in (a), (c), (e), and (f) are smoothed time series using a 19-year Hanning filter. The dashed lines in (a) and (c) show the linear trends, and the dashed line in (f) is the smoothed PDO index.

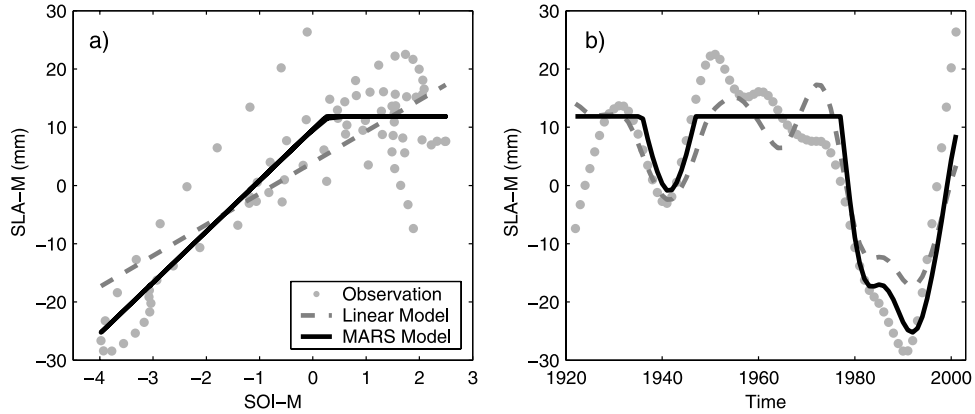

Figure 3. (a) Relationship between the SOI-M and the SLA-M, as well as the fitted values from the linear and MARS models, and (b) time series plot of observed SLA-M, and the linear and MARS fitted values.

SLA-M data is explained and the 95% confidence interval for the slope is estimated to be 5.34±1.14 mm per SOI-M unit. Note that on the ENSO time scale, the dependence of the Fremantle SLA on SOI has a slope of 4.5 mm per SOI unit [*Feng et al.*, 2003].

4. Non-parametric Piecewise Linear Regression Between SLA-M and SOI-M

[12] Now we use simplified multivariate adaptive regression spline (MARS) technique, a non-parametric piecewise linear model (Appendix), to describe the relationship between the SLA-M and SOI-M, with the expectation that we may capture more SLA-M variations. The fitted model is

$$Y_t = 11.86 - 8.76[0.26 - X_t]_+ + \varepsilon_t, \quad (3)$$

where $[\cdot]_+ = \max(0,\cdot)$ and ε_t is the residual, a second order autoregressive process. This non-parametric model explains 78% of the SLA-M variance, 9% higher than the linear model (Figure 3). It also describes a nonlinear relationship between the SLA-M and SOI-M: there is a linear relationship, with a slope of 8.76 mm per SOI-M unit, during the negative SOI-M regimes (Figure 3a). However, when the SOI-M is higher than 0.26, the SLA-M remains a constant at 11.86 mm. The nonlinearity described in equation 3 is significant at the 1% level based on a hypothesis test for segmented polynomial regression models [*Gallant and Fuller*, 1973].

[13] ENSO asymmetry is a likely cause of the nonlinearity. The annual mean Fremantle SLA tends to have a strong linear dependence on the SOI during the El Niño years, while during the La Niña years the relationship is not obvious (Figure 4). This asymmetry suggests that the sea level (upper-ocean) response to El Niño is stronger than that to La Niño at the same SOI level, which is reflected in the nonlinearity on the multidecadal time scale. Another type of ENSO asymmetry suggests that a certain heat content anomaly in the tropical Pacific could generate different amplitudes of air-sea coupling during the opposite ENSO phases [*Meinen and McPhaden*, 2000; *Cai et al.*, 2004]. The relationship between the two types of asymmetry needs further research.

5. Summary

[14] In this study, we have analyzed the multidecadal Fremantle sea level variability and related it to PDO-related multidecadal variations in the tropical Pacific. Similar to ENSO, the PDO-caused upper ocean anomalies transmit a high sea level anomaly at Fremantle during the positive SOI-M regime due to enhanced trade winds in the Pacific (e.g., 1950's—mid 1970's), and transmit a low sea level anomaly during the negative SOI-M regime due to slackened trade winds (e.g., mid 1970's—mid 1990's). Thus, the Fremantle sea level can be used as an index for low-frequency climate variability in the tropical Pacific. Recognition of the multidecadal variation in the Fremantle SLA helps explain its lower sea level rising trend compared to the global average value from 1950's to 1990's.

[15] To separate the sea level variation caused by the natural climate variability from that caused by climate change, we have explored statistical relationships between the SLA-M and SOI-M, via a linear regression model and a more sophisticated non-parametric piecewise linear regression technique based on MARS. While both models explain significant amounts of the SLA-M variance, the MARS model also reveals a nonlinear relationship between the

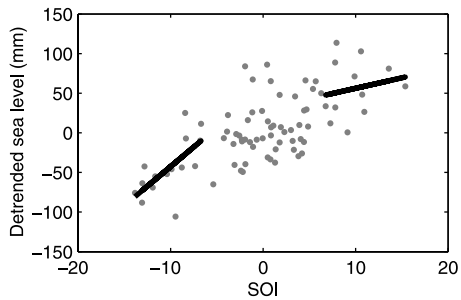

Figure 4. Scatter plot between the annual mean Fremantle SLA and SOI. Linear regressions are carried out when the annual mean SOI is greater than its standard deviation and are denoted with heavy lines.

SLA-M and the SOI-M: the SLA-M modulation is linearly related to the SOI-M during the negative SOI-M regime, while they have no obvious relationship during the positive SOI-M regime. Different sea level (upper-ocean) responses to the El Niño and La Niña events are hypothesized to be the cause of the nonlinearity.

Appendix A: Non-parametric Piecewise Linear Regression Based on MARS

[16] In general, a univariate nonlinear model can be written as

$$Y_t = f(X_t) + \varepsilon_t \tag{A1}$$

where f is an unknown function to be estimated from data and ε_t is the residual. The MARS approach of *Friedman* [1991], in a univariate regression case, can be written as:

$$\hat{f}(x) = \sum_{i=1}^{k} \beta_i B_i(x), \tag{A2}$$

where x is an observation of X_t and β_i ($i = 1,\ldots, k$) are statistically chosen coefficients of the basis functions B_i and k is the number of basis functions in the model. The B_i are given by

$$B_i(x) = \begin{cases} 1, & i = 1 \\ [s_i(x - t_i)]_+ & i = 2,\ 3, \ldots \end{cases} \tag{A3}$$

where $[\cdot]_+ = \max(0, \cdot)$, $s_i = \pm 1$ and t_i are knot positions.

[17] **Acknowledgments.** This work was supported by the Strategic Research Fund for the Marine Environment. We thank Wenju Cai, Eddy Campbell, John Church, Stuart Godfrey, Charitha Pattiaratchi, Quanxi Shao, Susan Wijffels, and Xiaogu Zheng for providing helpful advice. We also thank two anonymous reviewers for constructive comments.

References

Allan, R. J., J. A. Lindesay, and C. J. C. Reason (1995), Multidecadal variability in the climate system over the Indian Ocean region during the Austral summer, *J. Clim.*, *8*, 1853–1873.

Cai, W., M. J. McPhaden, and M. A. Collier (2004), Multidecadal fluctuations in the relationship between equatorial Pacific heat content anomalies and ENSO amplitude, *Geophys. Res. Lett.*, *31*, L01201, doi:10.1029/2003GL018714.

Church, J., N. J. White, R. Coleman, K. Lambeck, and J. X. Mitrovica (2004), Estimates of the regional distribution of sea-level rise over the 1950 to 2000 period, *J. Clim.*, in press.

Feng, M., and G. Meyers (2002), Interannual variation in the tropical Indian Ocean, A two-year time scale of the IOD, *Deep Sea Res. II*, *50*, 2263–2284.

Feng, M., G. Meyers, A. Pearce, and S. Wijffels (2003), Annual and interannual variations of the Leeuwin Current at 32°S, *J. Geophys. Res.*, *108*, 3355, doi:10.1029/2002JC001763.

Friedman, J. H. (1991), Multivariate adaptive regression splines (with discussion), *Am. Stat.*, *19*, 1–141.

Gallant, A. R., and W. A. Fuller (1973), Fitting segmented polynomial regression models whose join points have to be estimated, *J. Am. Stat. Assoc.*, *68*, 144–147.

Godfrey, J. S. (1996), The effect of the Indonesian throughflow on ocean circulation and heat exchange with the atmosphere: A review, *J. Geophys. Res.*, *101*, 12,217–12,235.

Gu, D.-F., and S. G. H. Philander (1995), Secular changes of annual and interannual variability in the tropics during the past century, *J. Clim.*, *8*, 864–876.

Holgate, S. J., and P. L. Woodworth (2004), Evidence for enhanced coastal sea level rise during the 1990s, *Geophys. Res. Lett.*, *31*, L07305, doi:10.1029/2004GL019626.

Jones, P. D., M. New, D. E. Parker, S. Martin, and I. G. Rigor (1999), Surface air temperature and its changes over the past 150 years, *Rev. Geophys.*, *37*, 173–199.

Kalnay, E., et al. (1996), The NCEP/NCAR 40-year reanalysis project, *Bull. Am. Meteorol. Soc.*, *77*, 437–471.

Lambeck, K. (2002), Ice sheets, sea level and the dynamic earth, in *Ice Sheets, Sea Level and the Dynamic Earth*, *Geodyn. Ser.*, vol. 29, edited by J. X. Mitrovica and B. L. A. Vermeersen, pp. 33–50, AGU, Washington, D.C.

Meinen, C. S., and M. J. McPhaden (2000), Observations of warm water volume changes in the equatorial Pacific and their relationship to El Niño and La Niña, *J. Clim.*, *13*, 3551–3559.

Meyers, G. (1996), Variation of Indonesian throughflow and the El Niño-Southern Oscillation, *J. Geophys. Res.*, *101*, 12,255–12,263.

Pariwono, J. I., J. A. T. Bye, and G. W. Lennon (1986), Long-period variations of sea level in Australia, *Geophys. J. R. Astron. Soc.*, *87*, 43–54.

Rodgers, K., P. Friederichs, and M. Latif (2004), Decadal ENSO amplitude modulation their effect on the mean state, *J. Clim.*, in press.

White, W. B., and R. L. Bernstein (1979), Design of an oceanographic network in the mid-latitude North Pacific, *J. Phys. Oceanogr.*, *9*, 592–606.

Zhang, Y., J. M. Wallace, and D. S. Battisti (1997), ENSO-like interdecadal variability: 1900–1993, *J. Clim.*, *10*, 1004–1020.

Zheng, X., R. E. Basher, and C. S. Thompson (1997), Trend detection in regional-mean temperature series: Maximum, minimum, mean, diurnal range, and SST, *J. Clim.*, *10*, 317–326.

M. Feng, CSIRO Marine Research, Floreat, WA 6014, Australia. (Ming.Feng@csiro.au)

Y. Li, CSIRO Mathematical and Information Sciences, Wembley, WA 6913, Australia.

G. Meyers, CSIRO Marine Research, GPO Box 1538, Hobart, TAS 7001, Australia.